I&EC research
Industrial & Engineering Chemistry Research

Article

pubs.acs.org/IECR

Investigation of Influencing Factors and Mechanism of Antimony and Arsenic Removal by Electrocoagulation Using Fe−Al Electrodes

Peipei Song, Zhaohui Yang,* Haiyin Xu, Jing Huang, Xia Yang, and Like Wang

College of Environmental Science and Engineering and Key Laboratory of Environmental Biology and Pollution Control, Ministry of Education, Hunan University, Changsha 410082, China

Supporting Information

ABSTRACT: Exposure to antimony (Sb) and arsenic (As) through contaminated surface water poses a great threat to human health. In this work, Sb and As were removed simultaneously by electrocoagulation (EC) using Fe−Al electrodes. The effects of current density, pH, initial concentration, aeration intensity, and anions were investigated. A higher current density achieved better removal performance. The optimum pH range was 5.0−7.0. Sb and As removals were slower at higher initial concentrations. Preoxidation was beneficial to As removal, whereas anoxic conditions were more favorable for Sb removal. Nitrate and sulfate had little influence on the performance of the EC process, but significant inhibition was observed in phosphate-rich solutions. Scanning electron microscopy/energy-dispersive spectroscopy (SEM/EDS), X-ray diffraction (XRD), and Fourier transform infrared (FTIR) analysis demonstrated that adsorption onto iron and aluminum hydroxides/oxyhydroxides was the predominant mechanism involved in Sb and As removal. Finally, over 99% of Sb and As were removed from a practical wastewater sample, indicating that EC using Fe−Al electrodes provides an alternative method for Sb and As removal.

1. INTRODUCTION

Antimony (Sb) and arsenic (As), two toxic metalloids, pose a major unavoidable threat to human health. Both Sb and As belong to group VA of the periodic table, and they are often considered to behave similarly and coexist with each other in the environment.[1,2] It has been reported that Sb and As can be released into surface water through various natural and anthropogenic processes, especially mining and smelting. For example, Xikuangshan, located near Lengshuijiang City, Hunan Province, China, has long been designated as the "World Antimony Capital", with approximately 90% of the total world production of 187000 t/year.[3] In the Xikuangshan Sb mine, associated with As mineralization, a series of deposit containing both Sb and As were formed.[4] Owing to excessive and indiscriminate digging, historical problems, and other anthropogenic effects, untreated ore tailings, smelter clinkers, and smelting residues were piled up in the open air near this mine. In the case of rainwash, large quantities of Sb and As are released into rivers and lakes, leading to a serious surface water pollution.[4]

Both Sb and As are highly toxic and persist in the environment. Sb irritates the eyes, nose, throat, and skin of people, and long-term exposure to Sb can damage the heart and liver function.[5] Arsenic is a carcinogen, and its consumption negatively affects the cardiovascular, gastrointestinal, reproductive, and central nervous systems even at low concentrations.[6] To minimize these risks, Sb and As have been listed as prime pollutants by U.S. Environmental Protection Agency (EPA)[7] and the Council of European Communities.[8] In addition, the U.S. EPA has established maximum permissible concentrations in drinking water of 6 μg/L for Sb and 10 μg/L for As.[9] In China, the national drinking water contaminant standards for Sb and As are set as 5 and 10 μg/L, respectively,[10] which are identical to the guidelines of the World Health Organization.[11] Therefore, it is necessary to find effective technologies to meet these regulations.

Recently, arsenic removal from wastewater has received extensive attention. A variety of methods including adsorption,[12,13] biological processing,[14,15] and chemical coagulation[16,17] have been developed. In contrast to the extensive research on As removal, Sb removal has received relatively little attention.[18,19] However, a sparsity of data on the simultaneous removal of Sb and As from contaminated surface water is strikingly evident.[20,21] The disadvantages of the methods mentioned above are that they require several pH adjustments and the addition of coagulants such as ferric sulfate, lime, or polymeric flocculants.[22,23] Some processes generate large quantities of secondary pollutants that pose a great threat to the environment. In recent years, electrocoagulation (EC) has shown the greatest potential for application with high removal efficiency, small production of sludge, no addition of chemicals, and the possibility of complete automation.[24,25] EC has been reported to be efficient in the treatment of different wastewaters such as textile wastewater,[26] restaurant wastewater,[27] chemical mechanical polishing (CMP) wastewater,[28] and especially heavy-metal-contaminated water.[29,30]

In an EC reactor, metal plates, such as aluminum or iron, are often used as electrodes. When a direct current is applied, the sacrificial anodes dissolve, and metallic cations such as Al^{3+}, Fe^{2+}, or Fe^{3+} are generated by the oxidation of the sacrificial anodes as follows[31,32]

Received: April 26, 2014
Revised: July 23, 2014
Accepted: July 24, 2014
Published: July 24, 2014

dx.doi.org/10.1021/ie501727a | Ind. Eng. Chem. Res. 2014, 53, 12911−12919

$$Al(s) - 3e^- \rightarrow Al^{3+}(aq) \quad (1)$$

$$Fe(s) - 2e^- \rightarrow Fe^{2+}(aq) \quad (2)$$

$$Fe^{2+}(aq) - e^- \rightarrow Fe^{3+}(aq) \quad (3)$$

When air (or oxygen) is introduced into the process, the following reaction occurs

$$O_2(g) + 4Fe^{2+}(aq) + 2H_2O(aq) \rightarrow 4Fe^{3+}(aq) + 4OH^-(aq) \quad (4)$$

At the cathode, production of H_2 typically occurs

$$2H_2O(aq) + 2e^- \rightarrow H_2(g) + 2OH^-(aq) \quad (5)$$

Generally, the Al^{3+}, Fe^{2+}, or Fe^{3+} ions released from the anode are gradually hydrolyzed and spontaneously form a range of coagulant species or metal hydroxides that absorb or coprecipitate with the dissolved pollutants. Simultaneously, the bubbles at the cathode capture and float the suspended solids, resulting in additional removal of contaminants.[33]

It has been noted that numerous factors such as pH, oxidation state, and electrode materials influence Sb and As removals by EC.[34] pH was reported to influence the species distribution and the surface charges of Sb, As, and metal oxides.[35,36] Studies have indicated that oxidation state affects the behavior of Sb and As removals in wastewater treatment systems.[37,38] Different electrode materials have different electrochemical characteristics, and appropriate electrode materials can improve treatment efficiency significantly.[35] In previous studies, EC with Fe or Al electrodes alone has already drawn considerable attention.[34,39] However, only a few reports have been published[35] about combined Fe−Al electrodes, which might provide an alternative method for the efficient removals of Sb and As from wastewater.

In the present study, Sb and As were removed simultaneously from contaminated surface water by EC using Fe−Al electrodes. Laboratory experiments quantified the effects of current density, pH, concentration, aeration intensity, and anions on the removals of Sb and As. In addition, the EC products were characterized by scanning electron microscopy/energy-dispersive spectroscopy (SEM/EDS), X-ray diffraction (XRD) and Fourier transform infrared (FTIR) spectroscopy to explore the removal mechanism of Sb and As. Furthermore, practical wastewater samples from Xikuangshan surface water were also analyzed to examine the performance of Sb and As removals.

2. MATERIAL AND METHODS

2.1. Materials. All of the chemicals used in this study were of guaranteed reagent (GR) grade. A 1000 mg/L Sb stock solution was prepared from antimony potassium tartrate ($KSbC_4H_4O_7 \cdot {}^1/_2H_2O$) dissolved in 20% (v/v) HCl. A stock synthetic solution of 1000 mg/L arsenic was prepared according to the EPA standard method by dissolving As_2O_3 in a solution containing 20% (w/v) KOH, neutralizing with 20% (v/v) H_2SO_4 to a phenolphthalein end point, and then diluting to 1000 mL with 1% (v/v) H_2SO_4. Simulated wastewaters containing 200−1000 μg/L Sb and As were prepared by diluting the above stock solutions. Phosphate, nitrate, and sulfate stock solutions were prepared from $Na_3PO_4 \cdot 12H_2O$, $NaNO_3$, and $NaSO_4$, respectively. To investigate the effects of initial pH, the treated water was adjusted to the desired pH with 0.1 mol/L HCl and 0.1 mol/L NaOH. All solutions were prepared with ultrapure water. Samples of practical wastewater were taken from the area of Xikuangshan Sb mines. All glassware, polyethylene bottles, and sample vessels were immersed in 5% (v/v) HNO_3 and rinsed with distilled water.

2.2. Experimental Setup. The EC experiments were carried out in batch mode using a 4 L plexiglas reactor (200 mm × 160 mm × 125 mm). Four plates (Fe, 99.5% purity; Al, 99.3% purity; 150 mm × 150 mm × 1 mm) vertically positioned in the aqueous solution were placed 2 cm apart. Anodes and cathodes were in serial connection in monopolar mode (MP-S). The submerged surface area of each electrode was 120 cm^2. Current density was adjusted with a dc power supply to the desired value (2.78−55.56 A/m^2).

2.3. Procedure. Before each trial, the electrodes were abraded with sand paper and then cleaned with 1 mol/L HNO_3 and deionized water. For each experiment, 2.5 L of Sb and As solution was added into the EC reactor. During each experiment, the pH, voltage, and conductivity were recorded. Ten milliliters of solution was collected every 5 min and then filtered with a 0.45-μm filter membrane for analysis. Duplicate runs were carried out for each set of experimental conditions. The remaining precipitated solids (EC products) were collected and dried in preparation for solid-phase characterization.

2.4. Analysis. EC products were characterized by SEM (Quanta 200 FEG, FEI, Hillsboro, OR). The elemental composition of EC products was analyzed by EDS. XRD analysis was carried out with a Bruker D8 diffractometer operating with a Cu Kα radiation source filtered with a graphite monochromator (λ = 1.54058 Å). The samples were ground to a fine powder and loaded into a sample holder. Powder specimens were filtered with 400-mesh sieves before X-ray diffraction analysis. The XRD scans were recorded from 10° to 80° 2θ with a 0.020° step width and a 6-s counting time for each step. FTIR analysis was carried out on an FTIR-8400S IR prestige-21 spectrometer using potassium bromide pellets. The spectra were recorded in the range of 4000−400 cm^{-1} with 2 cm^{-1} resolution, and 32 scans were collected for each specimen. Concentrations of Sb and As were measured by atomic fluorescence spectrophotometry (AFS) (Haiguang AFS-9760, Beijing).[40] Fe and Al analyses were performed using the flame atomic absorption spectrometer (FAAS) (Perkin-Elmer AA700, Wellesley, MA).[40] Concentrations of NO_3^-, SO_4^{2-}, Cl^-, and PO_4^{3-} were determined by ion chromatography (IC) (Dionex ICS-900, Sunnyvale, CA).[40]

3. RESULTS AND DISCUSSION

3.1. Factors Influencing Sb and As Removals. *3.1.1. Electrode Materials.* In this study, the effects of Fe−Fe, Al−Al, and Fe−Al electrodes on the removals of Sb and As were investigated. Fe−Al electrodes exhibited higher removal efficiencies than Al−Al and Fe−Fe electrodes (Table 1). Gomes et al.[35] observed the substitution of Fe^{3+} ions by Al^{3+} ions in the solid surface during the EC process with Fe−Al electrodes. Al^{3+} substitution slowed the transformation of amorphous iron hydroxide/oxyhydroxide species to the crystalline phase and resulted in a larger surface area of the total oxide mineral, which increased the adsorption of pollutants.[35] Therefore, our subsequent experiments focused on only Fe−Al electrodes.

3.1.2. Current Density. Current density is one of the most important operating parameters in the EC process. With an

Table 1. Results of Sb and As Removals with Different Electrode Materials[a]

electrode	current density (A/m^2)	pH	20-min treatment time: Sb removal efficiency (%)	20-min treatment time: As removal efficiency (%)	40-min treatment time: Sb removal efficiency (%)	40-min treatment time: As removal efficiency (%)
Fe−Fe	13.89	5	63.58	79.38	86.21	98.94
		7	60.24	82.17	80.84	99.31
		9	56.97	73.27	74.21	96.93
Al−Al	13.89	5	49.56	61.79	79.05	86.06
		7	43.27	69.74	71.56	89.31
		9	39.97	54.21	61.02	80.03
Fe−Al	13.89	5	67.03	83.47	93.36	99.26
		7	64.39	88.35	88.22	99.82
		9	59.87	79.86	80.27	98.47

[a]Initial concentration of each Sb and As: 500 μg/L.

increase in current density, the treatment time required to achieve a stable concentration was reduced, and the removal efficiencies of Sb and As improved (Figure 1a,b). This can be attributed to the fact that, at higher current density, an accumulation of hydroxide cationic complexes[41,42] is caused by the increased anodic metal dissolution in accordance with Faraday's law[32]

$$C_{theo} = It_{EC}M/ZFV \quad (6)$$

where C_{theo} (kg/m^3) is the theoretical amount of ion produced by current I (A) passed for a duration of operating time (s), Z is the number of electrons (Z_{Fe} = 2, Z_{Al} = 3), M is the atomic weight (M_{Fe} = 55.85 g/mol, M_{Al} = 26.98 g/mol), F is the Faraday constant (96485 C/mol), and V is the volume (m^{-3}) of water treated. The current density determines the coagulant dosage rate, the bubble production rate, and the size and growth of flocs, which can influence removal efficiencies of Sb and As.[41] As a result, in the early stage of the EC process, a clear positive correlation was observed between the current density and the removal efficiencies of Sb and As.

However, the same plateau was obtained when the current density was greater than 13.89 A/m^2. There was no significant correlation between the final removal efficiency and the current density. This observation can be explained by the fact that the final removal efficiency is associated with the amount of coagulant, which is directly governed by the charge density[42,43]

$$Q = It_{EC}/FV \quad (7)$$

where the charge density Q (C/m^3) is calculated as the current I (A) applied in the EC process multiplied by the operating time t_{EC} (s) per unit of volume V (m^{-3}), divided by the Faraday constant (F = 96485 C/mol). The results obtained at different

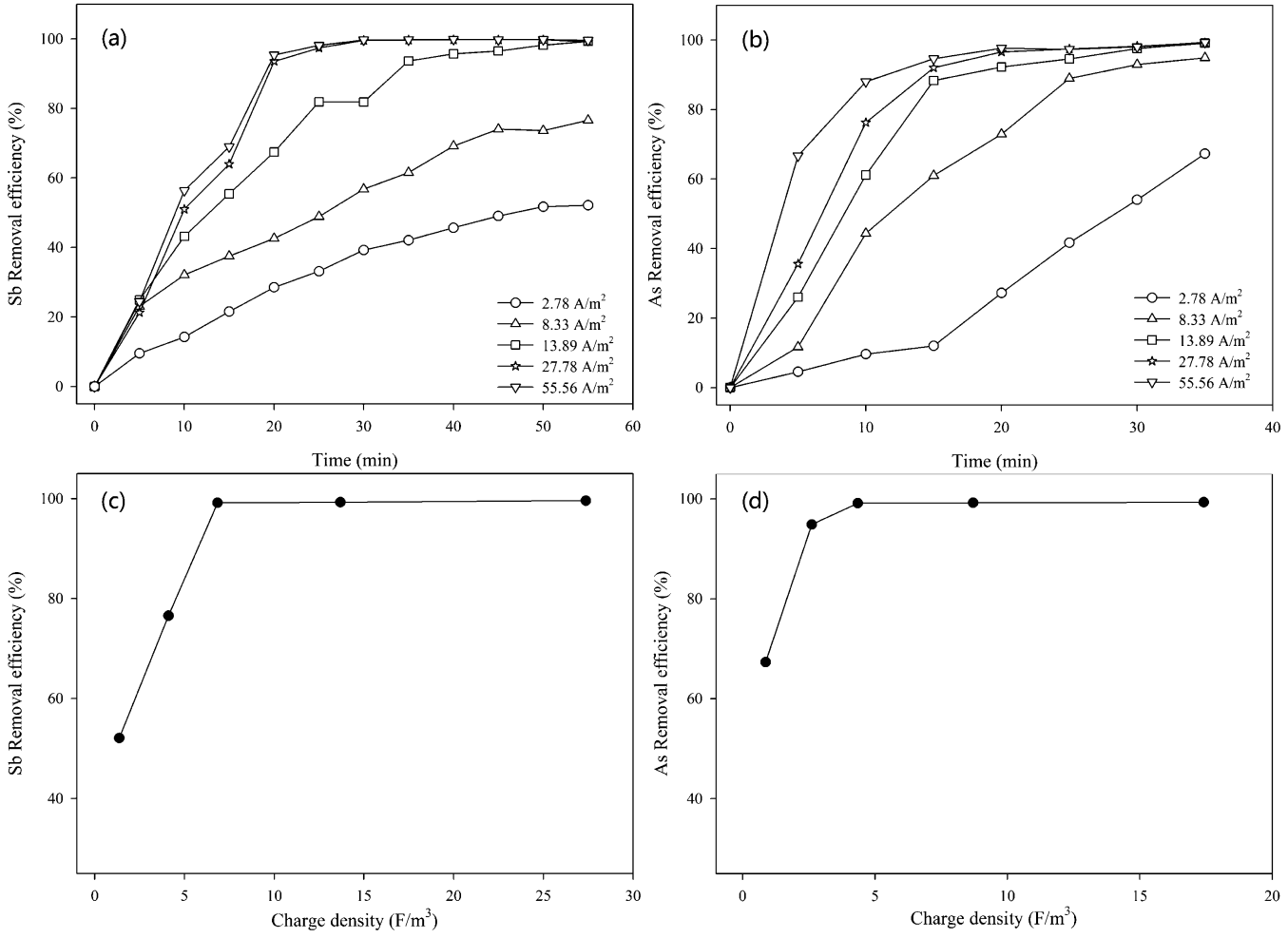

Figure 1. Effects of (a,b) current density and (c,d) charge density on (a,c) Sb and (b,d) As removals in the EC process (initial concentration of each Sb and As, 500 μg/L; time for Sb, 55 min; time for As, 35 min).

dx.doi.org/10.1021/ie501727a | Ind. Eng. Chem. Res. 2014, 53, 12911−12919

current densities were converted into charge densities, as shown in Figure 1c,d. When the charge density was low, the coagulant dosages of typical iron and aluminum hydroxides/oxyhydroxides were not sufficient to remove Sb and As, and thus the final removal efficiencies were not high. Once the coagulant dosage was sufficient, the final removal efficiencies reached a constant value. This implies that the charge density could serve as an important design parameter in the EC process.[31,44] When the current density was greater than 13.89 A/m^2, the results were suitable for all cases where the Sb and As concentrations were lower than the permissible level. Considering operating costs, all further experiments were performed at a current density value of 13.89 A/m^2.

3.1.3. Initial pH. As shown in Figure 2a,b, the optimum pH range for Sb and As removals was observed at 5.0−7.0. This result might be related to the forms of Sb, As, Fe, and Al existing at different pH values.[35] As shown in Figure 3, Sb(III) existed as a neutral species over a wide range of pH. For Sb(V), at pH > 5, $Sb(OH)_6^-$ dominated in bulk solution. Meanwhile, the ratio of positively charged $Fe(OH)_3$ and $Al(OH)_3$ colloidal particles reached the maximum value. As a result, higher Sb removal efficiency was achieved due to electrical neutralization. With respect to As, when the solution was neutral, for As(III), the amount of neutral molecule H_3AsO_3 decreased, whereas the amount of negatively charged $H_2AsO_3^-$ increased. For As(V), the amount of $H_2AsO_4^-$ decreased, whereas the amount of $HAsO_4^{2-}$ increased. Moreover, $Fe(OH)_2$ formed, and the ratio of positively charged $Fe(OH)_3$ and $Al(OH)_3$ colloidal particles reached the maximum value. Hence, the optimal As removal efficiency was obtained. For pH > 9, the ratio of $Al(OH)_3$ and $Fe(OH)_3$ decreased, and $Al(OH)_4^-$ and $Fe(OH)_4^-$ were generated (eqs 8 and 10). Moreover, both Sb and As species were negatively charged, and the adsorption was less favorable. As a result, the removal efficiencies of Sb and As decreased.

Finally, at pH 3.0−9.0, high removal efficiencies of both Sb and As were obtained (Figure 2a,b), indicating that EC can work effectively over a wide pH range. The concentrations remaining in solution were below the allowable limit when the treatment time was longer than 60 min for Sb and 35 min for As. Figure 2c displays variations in the initial and final pH values during the EC process. As the initial pH rose from 3.0 to 7.0, there was an obvious increase in final pH, which was caused by the production of hydrogen gas and hydroxyl ions (OH^-) at the cathode (eq 6). Accordingly, the electrolytic reactor was capable of producing sufficient OH^- ions to compensate for the acid buffer and make the solution alkaline.[33] However, when the initial pH was 9.0−11.0, the final pH decreased. At high pH, considering that $Fe(OH)_3$ and $Al(OH)_3$ are typical amphoteric metal hydroxides, reactions 8−10 could take place, leading to a decline in pH. Based on the above phenomenon, one can conclude that EC could act by neutralizing pH. It could eliminate further pH adjustment of the effluent, which is meaningful to the application of EC.[27]

$$Fe(OH)_3(s) + OH^-(aq) \rightarrow Fe(OH)_4^-(aq) \quad (8)$$

$$Fe(OH)_4^-(aq) + 2OH^-(aq) \rightarrow Fe(OH)_6^{3-}(aq) \quad (9)$$

$$Al(OH)_3(s) + OH^-(aq) \rightarrow Al(OH)_4^-(aq) \quad (10)$$

3.1.4. Initial Concentration. The effects of initial concentration ranging from 200 to 1000 μg/L were examined at pH 5.0 for Sb and at pH 7.0 for As. It took more time to get below the limits for Sb and As when the solutions had higher initial

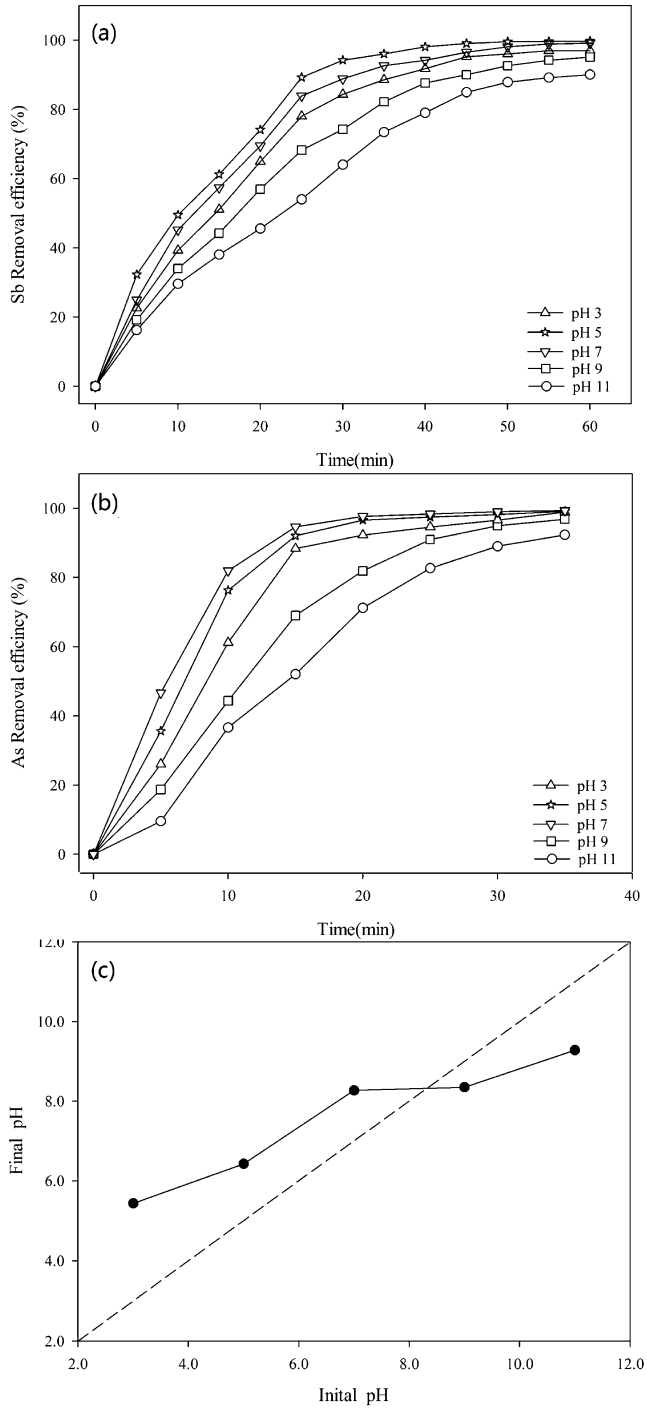

Figure 2. (a,b) Effects of initial pH on (a) Sb and (b) As removals and (c) comparison of initial and final pH values in the EC process (initial concentration of each Sb and As, 500 μg/L).

concentrations (Table 2). This result can be potentially explained by the fact that, when the initial concentrations were higher, more metallic hydroxides/oxyhydroxides were needed to reduce the dissolved Sb and As.[43] Sb and As removals were consequently limited by the production rate of metallic hydroxides.[36] Table 2 also shows that As removal was easier than Sb removal at different initial concentrations. As shown in Figure 3, at pH values ranging from 3 to 11, Sb(III) had a limited solubility in solution,[20] and it existed as the neutral molecule H_3SbO_3 in solutions with pH values ranging

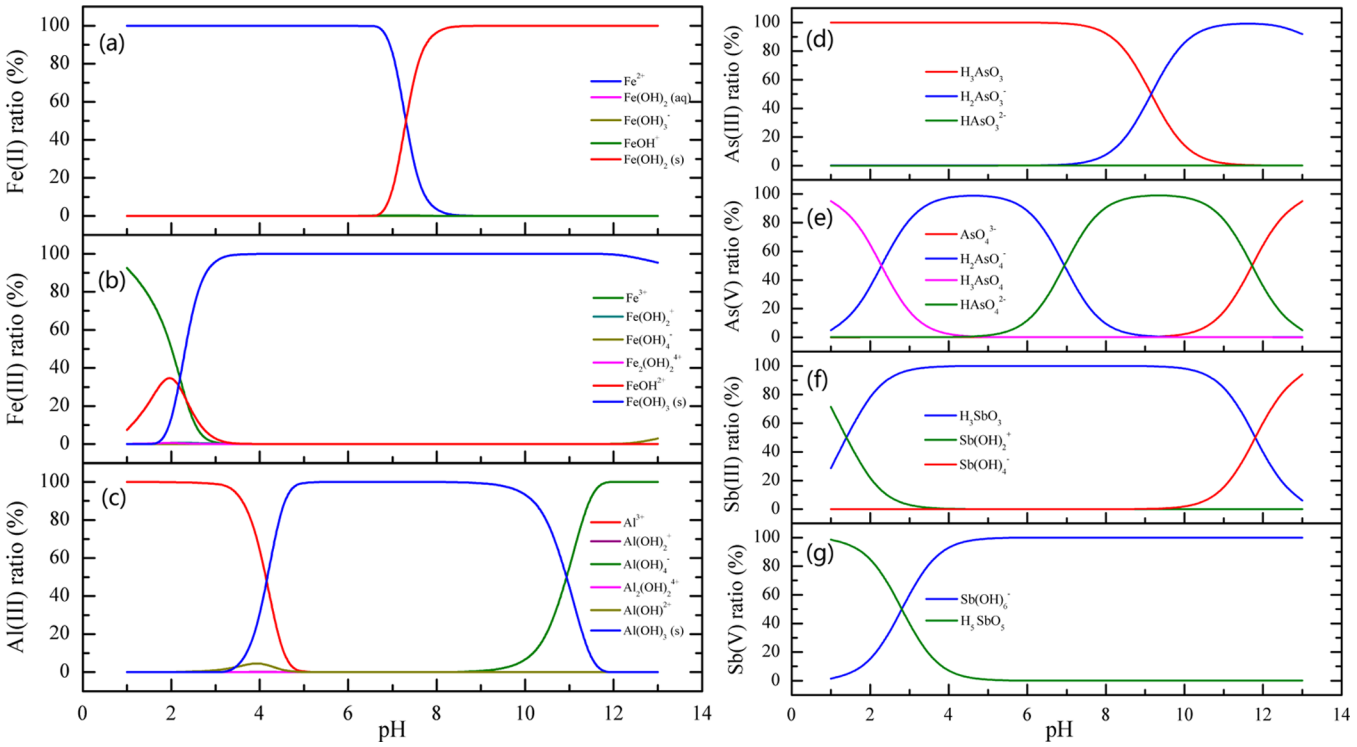

Figure 3. Predominance zone diagrams for the species of (a) Fe(II), (b) Fe(III), (c) Al(III), (d) As(III), (e) As(V), (f) Sb(III), and (g) Sb(V) in solutions simulated by Visual MINTEQ version 3.0.

Table 2. Results of Sb and As Removals with Different Initial Concentrations[a]

		Sb removal efficiency (%)			As removal efficiency (%)		
initial conc (μg/L)	current density (A/m^2)	25 min	50 min	95 min	15 min	30 min	65 min
200	13.89	98.01	>99.96	>99.96	96.68	>99.96	>99.96
500	13.89	71.26	98.13	>99.98	81.19	93.82	>99.98
1000	13.89	43.19	79.56	98.61	38.96	64.23	92.34

[a]Detection limit for Sb and As was 0.09 μg/L.

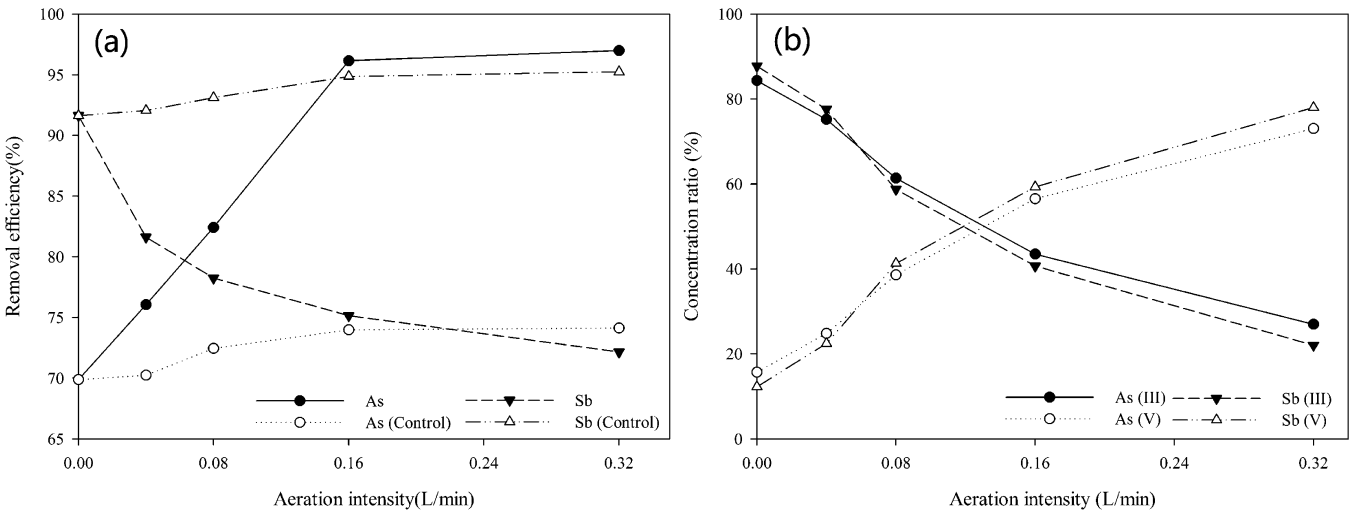

Figure 4. Effects of aeration intensity on the (a) removal efficiency and (b) variation in valence states of As and Sb in the EC process (initial concentration of each Sb and As, 500 μg/L).

from 2 to 11. Sb(V) was proposed to have one negative charge of $Sb(OH)_6^-$ in aqueous solution. For As(III), the predominant species were H_3AsO_3 at pH values of 3−9 and $H_2AsO_3^-$ at pH values of 9−11. As(V) was mainly in the form of $H_2AsO_4^-$ at pH values of 3−7 and $HAsO_4^{2-}$ at pH values of 7−11. Meanwhile, the surfaces of iron and aluminum hydroxides/oxyhydroxides colloidal particles were positively charged,[36] and the negative charge of As was greater than that of Sb. Because

dx.doi.org/10.1021/ie501727a | Ind. Eng. Chem. Res. 2014, 53, 12911−12919

of electrostatic attraction and chemical contributions,[36] arsenic adsorption was thus found to be more favorable than Sb adsorption.

3.1.5. Aeration Intensity. In these experiments, the solution was sparged with pure oxygen, and the control experiment was conducted with nitrogen. As shown in Figure 4a, with aeration intensity increasing from 0 to 0.16 L/min, arsenic removal increased sharply, and when the aeration intensity was greater than 0.16 L/min, it approached a constant value. However, the opposite trend was obtained in Sb removal. Although the chemistry of Sb is similar to that of As, as both Sb and As are metalloids in group V of the periodic table,[45] Sb presented apparent dissimilarities from As with different aeration intensities in this study. Both Sb and As have two valence states: trivalence and pentavalence. With increasing aeration intensity, As(III) and Sb(III) were favorably converted into As(V) and Sb(V), respectively (Figure 4b). As demonstrated in previous studies,[31,35,46] As(V) can be removed more easily than As(III) because of different species existing in solution, as shown in Figure 3. Moreover, under aeration conditions, Fe^{2+} separated out at the anode was oxidized into Fe^{3+}, whose capacity for forming hydrate is stronger. Furthermore, aeration provided the necessary turbulent current conditions for the flocs to contact and collide, ultimately resulting in much better removal performance. In contrast to As removal, Sb(V) removal is more difficult than Sb(III) removal, which might be due to the low adsorption enthalpy of Sb(V) for iron or aluminum hydroxides/oxyhydroxides,[19,46] so the tendency of Sb removal exhibited a distinct difference. This was in agreement with the results reported in a previous study on Sb removal.[46] In summary, both Sb and As removals by EC were sensitive to aeration intensity, and preoxidation was in favor of As removal, whereas anoxic conditions were helpful to Sb removal.[46]

3.1.6. Anions. $NaNO_3$, Na_2SO_4, and $Na_2HPO_4{\cdot}7H_2O$ were added to the treated water to evaluate the effects of nitrate, sulfate, and phosphate, respectively, on the removals of Sb and As. As observed in Figure 5, the presence of 1 and 5 mg/L nitrate had little effect on the final removal efficiencies of Sb and As, and the same was true for solutions containing sulfate, because the formation of iron and aluminum hydroxides/oxyhydroxides is not influenced by nitrate and sulfate.[47]

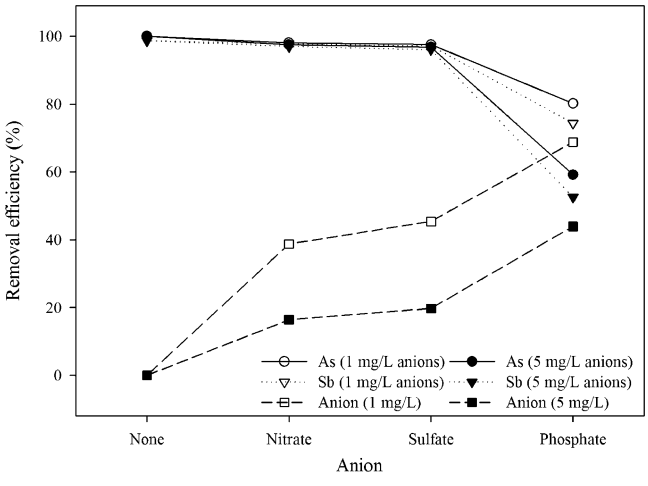

Figure 5. Removal efficiencies of As, Sb, and anions in the EC process (initial concentration of each Sb and As, 500 μg/L).

Although small amounts of nitrate and sulfate were removed, they were not adsorbed as strongly as Sb and As were. However, the presence of 1 and 5 mg/L phosphate inhibited the removals of Sb and As, and the inhibitory effect was more significant at higher phosphate concentrations. Meanwhile, large amounts of phosphate were removed. Similar results were also observed in a study of As removal by ferric chloride.[47] First, the reason for this behavior is, in part, that phosphate possibly plays a competitive role in the adsorption of Sb and As.[36,48,49] Second, as described in a previous study,[36] the slower oxidation of ferrous to ferric ion in solutions containing phosphate reduced the rate at which the sorbent was formed. In addition, some researchers have even observed the presence of iron(III) phosphate solids during the oxidation of Fe(II) in phosphate-rich solutions.[50]

3.2. Mechanism Involved in Sb and As Removal. The surfaces of the EC products were analyzed by SEM, and the images displayed the presence of an ultrafine particular structure at micrometer size (Figure 6a,b). Energy-dispersive spectroscopy (EDS) confirmed the presence of Fe, Al, Sb, and As in the EC products, which confirmed the removals of Sb and As from the solution.

The possible mechanism of Sb and As removal includes precipitation, coprecipitation, and adsorption.[46] In this study, precipitation is used in a general way to describe any process resulting in the production of solids.[19] Coprecipitation is defined as the incorporation of soluble Sb and As species into a growing hydroxide phase through inclusion, occlusion, or adsorption.[19,46] (1) Inclusion includes two forms: isomorphic inclusion and nonisomorphic inclusion. In isomorphic inclusion, the impurity is substituted into the crystal lattice for a lattice ion of similar size and chemical characteristics. In nonisomorphic inclusion, the impurity appears to be dissolved in the precipitate. (2) In occlusion, an impurity differing in size or chemical characteristics from the lattice sites is incorporated as crystals are growing, producing crystal imperfections. (3) In adsorption, the impurity is not incorporated into the internal crystal structure, but rather the formation of surface complexes between soluble species and solid (hydroxide, in this case) surface sites occurs.

To explore the mechanism responsible for Sb and As removal by electrocoagulation, XRD and FTIR analyses of the EC products were carried out. If the precipitation mechanism occurs in Sb and As removal, either Sb–Fe(III)/Al or As–Fe(III)/Al precipitates should be observed. However, the XRD and FTIR analyses (Figure 6c,d and Table 3) revealed the presence of amorphous or poorly crystalline phases, such as lepidocrocite [FeO(OH)] and diaspora [AlO(OH)], and crystalline phases, typically magnetite (Fe_3O_4). No Sb–Fe(III)/Al or As–Fe(III)/Al precipitates were expected to form, in agreement with other reports.[19,36,46]

To investigate whether inclusion or occlusion is a functional mechanism responsible for Sb and As removal by EC, the degrees of Sb and As removal by EC were compared with adsorption of Sb and As onto preformed EC products. The preformed products were collected by treating distilled water instead of Sb and As solutions by EC under the same conditions. If inclusion or occlusion plays a leading role in the removal mechanism, EC should show a preferential removal. The experimental results indicated that 99.75% of As and 89.23% of Sb were removed by EC, whereas with performed EC products, the removal efficiencies of Sb and As were 86.47% and 68.52%, respectively. This is in agreement with the results

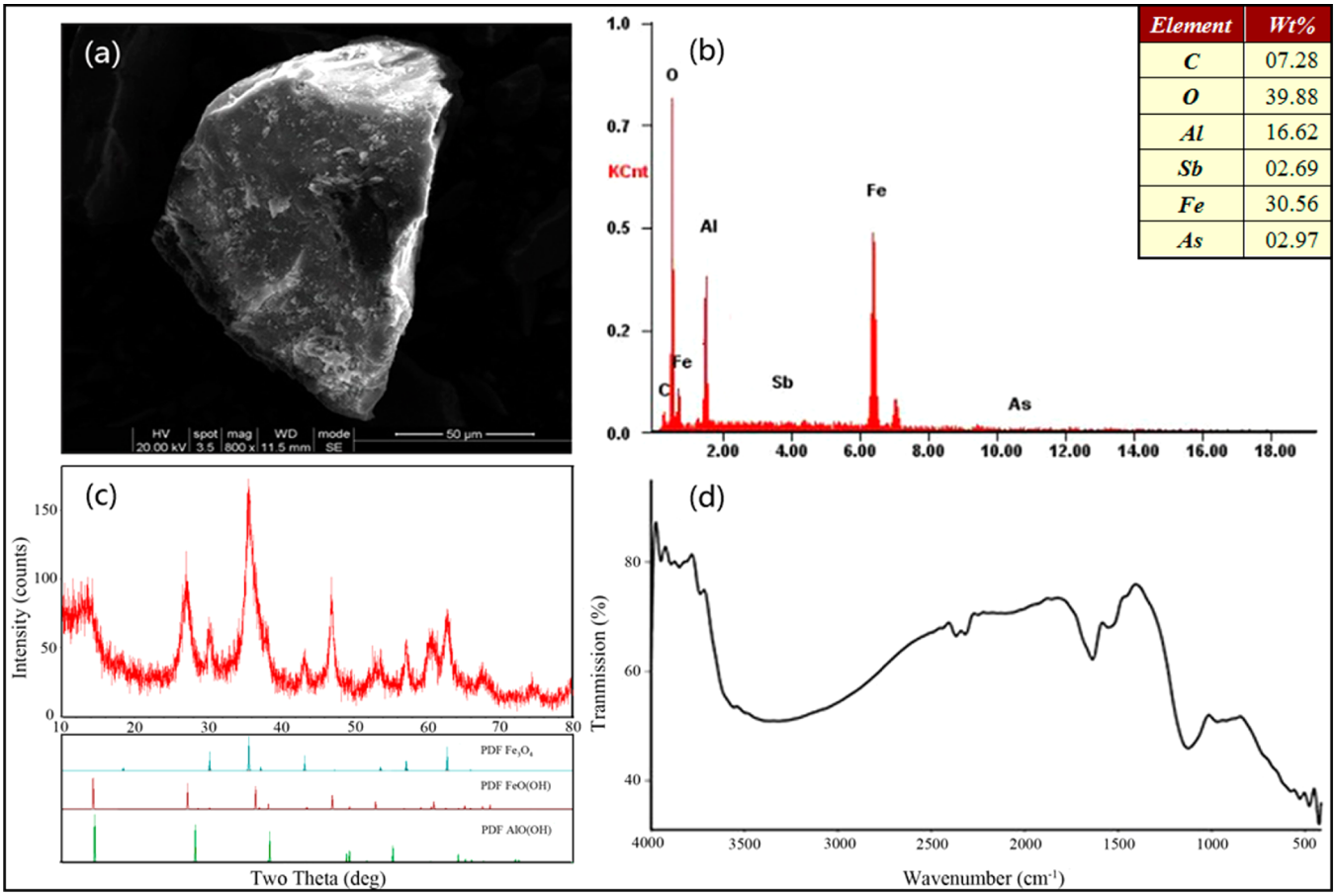

Figure 6. (a) SEM, (b) EDS, (c) XRD, and (d) FTIR analyses of EC products using Fe−Al electrodes.

Table 3. FTIR Vibrations, Corresponding Wavenumbers, and Ranges for the Bands Observed[35,51−53]

type of vibrations	vibration wavenumber(s) (cm^{-1})	vibration range (cm^{-1})
OH stretching for basic hydroxyl groups from aluminum hydroxides/ oxyhydroxides	3737, 3563	3530−3644
OH stretching for hydroxyl groups from iron oxyhydroxides	3496	3000−3550
hydroxyl bending	1638	1572−1813
γ′ (OH) water bending	1638	1572−1813
overtones of hydroxyl bending	1638	1572−1813
	1574	1572−1813
lepidocrocite	1131	1090−1245
	737	730−790
Al−O−H bending	975	880−1000
magnetite	575, 527	526−840
Fe−O	470, 420	416−510

reported by Guo et al. for Sb removal by coagulation−flocculation−sedimentation (CFS)[46] and by Song et al. for As removal by coagulation.[54] Therefore, inclusion or occlusion seem not to be a predominant mechanism, but adsorption onto iron and aluminum hydroxides/oxyhydroxides could be a possible removal mechanism.

3.3. Treatment of Practical Contaminated Surface Water. The practical wastewater samples collected from Xikuangshan Sb mine areas had high Sb and As concentrations and a small amount of phosphate (Table 4). Owing to low phosphate concentrations and sufficient treatment times, it was not surprising that no significant inhibition of treatment performance was observed in these trials. Despite the high initial concentrations of Sb and As, more than 99% of Sb and As were removed, and the concentrations of Sb and As remaining in the treated waters were far lower than the maximum permissible value. The phosphate concentrations were also below the detection limit of 10 μg/L. In addition, the concentrations of Fe^{3+} and Al^{3+} generated in the EC process were below the allowable limits. These results demonstrate that EC using Fe−Al electrodes is an effective and promising technology for treating wastewater contaminated with Sb and As.

4. CONCLUSIONS

(1) More than 99% of Sb and As were removed from simulated and practical wastewatesr, indicating that EC using Fe−Al electrodes provides an alternative method for the simultaneous removal of Sb and As from wastewater.

(2) In this work, the behaviors of Sb and As removal were discussed, and the optimum conditions of Sb and As removal were also explored. With an increase in current density from 2.78 to 13.89 A/m^2, there was a positive correlation between current density and the removals of Sb and As. However, beyond 13.89 A/m^2, the final removal efficiencies reached a constant value, which was possibly normalized with respect to the total charge passed. The optimum pH range for Sb and As removal was observed to be 5.0−7.0. The removals of Sb and As were slower at higher initial concentrations. At high aeration

dx.doi.org/10.1021/ie501727a | Ind. Eng. Chem. Res. 2014, 53, 12911−12919

Table 4. Concentrations of Sb, As, and PO_4^{3-} in Untreated and Treated Waters[a]

		initial conc (μg/L)			final conc[b] (μg/L)				removal efficiency (%)		
sample	pH	Sb	As	PO_4^{3-}	Sb	As	PO_4^{3-}	time (min)	Sb	As	PO_4^{3-}
1	7.36	762.43	312.16	258	4.98	nd	nd	75	99.35	>99.97	>96.12
2	7.98	568.24	284.56	189	4.24	nd	nd	65	99.25	>99.97	>94.71
3	7.59	421.88	182.87	121	3.97	nd	nd	50	99.06	>99.95	>91.74
4	8.28	932.65	553.47	396	4.83	nd	nd	95	99.48	>99.98	>97.47
5	8.02	768.42	376.98	202	4.04	nd	nd	85	99.47	>99.98	>95.05
6	7.79	821.72	443.41	352	4.89	nd	nd	85	99.40	>99.98	>97.16
7	7.62	385.36	202.95	164	2.68	nd	nd	45	99.30	>99.96	>93.90

[a]Current density = 13.89 A/m^2. [b]nd, not detected. The detection limits for As and PO_4^{3-} were 0.09 and 10 μg/L, respectively.

intensity, arsenic removal was preferred, but Sb removal declined. Nitrate and sulfate had little influence on the performance of the EC process. However, an inhibitory effect was observed in solutions containing phosphate. These experimental results can provide a theoretical basis for the further study and utilization of EC in the treatment of wastewaters contaminated with Sb and As.

(3) SEM/EDS, XRD, and FTIR analyses revealed the existence of amorphous or poorly crystalline phases, such as lepidocrocite [FeO(OH)] and diaspora [AlO(OH)], and crystalline phases, typically magnetite (Fe_3O_4). No Sb−Fe(III)/Al or As−Fe(III)/Al precipitates were expected to form. It was also confirmed that adsorption onto iron and aluminum hydroxides/oxyhydroxides was the main mechanism of Sb and As removal. However, more specific and detailed experiments in a subsequent study are required to explore the types of adsorption occurring.

■ ASSOCIATED CONTENT

Supporting Information

Theoretical concentration of Fe/Al in the EC process (current = 0.3 A) (Figure S1). Final concentrations of iron and aluminum in each experiment (Table S1). Concentrations of common cations, anions, Sb, and As in water samples collected from the Xikuangshan area (Table S2). This material is available free of charge via the Internet at http://pubs.acs.org.

■ AUTHOR INFORMATION

Corresponding Author

*E-mail: yzh@hnu.edu.cn. Tel.: +86-157-17484818. Fax: +86-731-88822829.

Notes

The authors declare no competing financial interest.

■ ACKNOWLEDGMENTS

We are grateful for the financial support of the National Natural Science Foundation of China (50478053) and the National Key Science and Technology Project for Water Environmental Pollution Control (2009ZX07212-001-02).

■ REFERENCES

(1) Filella, M.; Belzile, N.; Chen, Y. W. Antimony in the environment: A review focused on natural waters: I. Occurrence. *Earth-Sci. Rev.* **2002**, *57*, 125−176.

(2) Smedley, P. L.; Kinniburgh, D. G. A review of the source, behavior and distribution of arsenic in natural waters. *Appl. Geochem.* **2002**, *17*, 517−568.

(3) *Mineral Commodity Summaries 2010*; U.S. Geological Survey: Washington, DC, 2010.

(4) Tao, Y.; Jing, J. F. Paragenesis and differentiation of As, Au with Sb in Xikuangshan-type antimony deposits, central Hunan. *Mineral. Acta* **2001**, *21*, 67−72 (in Chinese).

(5) Smichowski, P.; Madrid, Y.; Cámara, C. Analytical methods for antimony speciation in waters at trace and ultratrace levels. A review. *Fresenius' J. Anal. Chem.* **1998**, *360*, 623−629.

(6) Wang, Z. X.; Chai, L. Y.; Wang, Y. Y. Potential health risk of arsenic and cadmium in groundwater near Xiangjiang River, China: A case study for risk assessment and management of toxic substances. *Environ. Monit. Assess.* **2011**, *175*, 167−173.

(7) *Water Related Fate of the 129 Priority Pollutants*; Report EPA 745-R-00-007; U.S. Environmental Protection Agency: Washington, DC, 1979.

(8) Council Directive 76/Substances Discharged into Aquatic Environment of the Community. *Off. J. Eur. Communities: Legis.* **1979**, *129*, 23−29.

(9) National Primary Drinking Water Regulations: Arsenic and Clarifications to Compliance and New Source Contaminants Monitoring. *Fed. Reg.*. **2001**, *66*, 6975−7066.

(10) *Standards for Drinking Water Quality*; Document GB-5749-2006; Standardization Administration of China: Beijing, 2006.

(11) *Guidelines for Drinking Water Quality*; World Health Organization: Geneva, Switzerland, 2006; Vol. *1*, p 306.

(12) Zhang, Y.; Yang, M.; Huang, X. Arsenic(V) removal with a Ce(IV)-doped iron oxide adsorbent. *Chemosphere* **2003**, *51*, 945−952.

(13) Katsoyiannis, I. A.; Zouboulis, A. I. Removal of arsenic from contaminated water sources by sorption onto iron-oxide-coated polymeric materials. *Water Res.* **2002**, *36*, 5145−5155.

(14) Katsoyiannis, I. A.; Zouboulis, A. I.; Althoff, H.; Bartel, H. As(III) removal from groundwaters using fixed bed upflow bioreactors. *Chemosphere* **2002**, *47*, 325−332.

(15) Katsoyiannis, I. A.; Zouboulis, A. I. Application of biological processes for the removal of arsenic from groundwaters. *Water Res.* **2004**, *38*, 17−26.

(16) Wickramasinghe, S. R.; Hana, B.; Zimbronb, J.; Shenc, Z.; Karima, M. N. Arsenic removal by coagulation and filtration: Comparison of ground waters from the United States and Bangladesh. *Desalination* **2004**, *169*, 231−244.

(17) Ciardell, M. C.; Xu, H. F.; Sahai, N. Role of Fe(II), phosphate, silicate, sulfate, and carbonate in arsenic uptake by coprecipitation in synthetic and natural groundwater. *Water Res.* **2008**, *42*, 615−624.

(18) Xu, G. M.; Shi, Z.; Deng, J. Characterization of iron oxide coated sand and its adsorption properties in antimony removal. *J. Environ. Sci.* **2006**, *26*, 607−612 (in Chinese).

(19) Kang, M.; Kamei, T.; Magara, Y. Comparing polyaluminum chloride and ferric chloride for antimony removal. *Water Res.* **2007**, *37*, 4171−4179.

(20) Kang, M.; Kawasaki, M.; Tamada, S. Effect of pH on the removal of arsenic and antimony using reverse osmosis membranes. *Desalination* **2000**, *131*, 293−298.

(21) Navarro, P.; Alguacil, F. J. Adsorption of antimony and arsenic from a copper electrorefining solution onto activated carbon. *Hydrometallurgy* **2002**, *66*, 101−105.

(22) Lakshmanan, D.; Clifford, D. A.; Samanta, G. Comparative study of arsenic removal by iron using electrocoagulation and chemical coagulation. *Water Res.* **2010**, *44*, 5641−5652.
(23) Holta, P. K.; Bartona, G. W.; Warka, M.; Mitchell, C. A. A quantitative comparison between chemical dosing and electrocoagulation. *Colloids Surf. A* **2002**, *211*, 233−248.
(24) Yousuf, M.; Mollah, A.; Schennach, R.; Parga, J. R. Electrocoagulation (EC)—Science and applications. *J. Hazard. Mater.* **2001**, *84*, 29−41.
(25) Mills, D. A new process for electrocoagulation. *J. Am. Water Works Assoc.* **2000**, *92*, 34−43.
(26) Kobya, M.; Can, O. T.; Bayramoglu, M. Treatment of textile wastewaters by electrocoagulation using iron and aluminum electrodes. *J. Hazard. Mater.* **2003**, *100*, 163−178.
(27) Chen, X. M.; Chen, G. H.; Yue, P. L. Separation of pollutants from restaurant wastewater by electrocoagulation. *Sep. Purif. Technol.* **2000**, *19*, 65−76.
(28) Lai, C. L.; Lin, S. H. Electrocoagulation of chemical mechanical polishing (CMP) wastewater from semiconductor fabrication. *Chem. Eng. J.* **2003**, *95*, 205−211.
(29) Akbal, F.; Camci, S. Copper, chromium and nickel removal from metal plating wastewater by electrocoagulation. *Desalination* **2011**, *269*, 214−222.
(30) Bhatti, M. S.; Reddy, A. S.; Kalia, R. K.; Thukral, A. K. Modeling and optimization of voltage and treatment time for electrocoagulation removal of hexavalent chromium. *Desalination* **2011**, *269*, 157−162.
(31) Kumar, P. R.; Chaudhari, S.; Khilar, K. C.; Mahajan, S. P. Removal of arsenic from water by electrocoagulation. *Chemosphere* **2004**, *55*, 1245−1252.
(32) Kobya, M.; Gebologlu, U.; Ulua, F.; Oncela, S. Removal of arsenic from drinking water by the electrocoagulation using Fe and Al electrodes. *Electrochim. Acta* **2011**, *56*, 5060−5070.
(33) Qu, J. H.; Liu, H. J. *Electrochemical Principles and Techniques in Water Treatment*; Science Press: Beijing, 2007; pp 205−209.
(34) Kumar, N. S.; Goel, S. Factors influencing arsenic and nitrate removal from drinking water in a continuous flow electrocoagulation (EC) process. *J. Hazard. Mater.* **2010**, *173*, 528−533.
(35) Gomes, J. A. G.; Daida, P.; Kesmez, M. Arsenic removal by electrocoagulation using combined Al−Fe electrode system and characterization of products. *J. Hazard. Mater.* **2007**, *139*, 220−231.
(36) Wan, W.; Pepping, T. J.; Banerji, T. Effects of water chemistry on arsenic removal from drinking water by electrocoagulation. *Water Res.* **2011**, *45*, 384−392.
(37) Quentel, F.; Filella, M.; Elleouet, C. Kinetic studies on Sb(III) oxidation by hydrogen peroxide in aqueous solution. *Environ. Sci. Technol.* **2004**, *38*, 2843−2848.
(38) Leuz, A. K.; Johnson, C. A. Oxidation of Sb(III) to Sb(V) by O_2 and H_2O_2 in aqueous solutions. *Geochim. Cosmochim. Acta* **2005**, *69*, 1165−1172.
(39) Zhu, J.; Wu, F. C.; Pan, X. L.; Guo, J. Y.; Wen, D. S. Removal of antimony from antimony mine flotation wastewater by electrocoagulation with aluminum electrodes. *J. Environ. Sci.* **2011**, *23*, 1066−1071.
(40) CEPA. *Water and Wastewater Monitoring Analysis Methods*, 4th ed.; China Environmental Science: Beijing, 2002.
(41) Kobya, M.; Demirbas, E.; Bayramoglu, M.; Sensoy, M. T. Optimization of Electrocoagulation Process for the Treatment of Metal Cutting Wastewaters with Response Surface Methodology. *Water, Air, Soil Pollut.* **2011**, *215*, 399−410.
(42) Flores, O. J.; Nava, J. L.; Carreño, G.; Elorza, E.; Martínez, F. Arsenic removal from groundwater by electrocoagulation in a pre-pilot-scale continuous filter press reactor. *Chem. Eng. Sci.* **2013**, *28*, 1−6.
(43) Kobya, M.; Ulu, F.; Gebologlu, U.; Demirbas, E. Treatment of potable water containing low concentration of arsenic with electrocoagulation: Different connection modes and Fe−Al electrodes. *Sep. Purif. Technol.* **2011**, *77*, 283−293.
(44) Vik, E. A.; Carlson, D. A.; Eikum, A. S.; Gjessing, E. T. Electrocoagulation of potable water. *Water Res.* **1984**, *18*, 1355−1360.
(45) Faust, S. D.; Aly, O. M. *Chemistry of Water Treatment*, 2nd ed.; CRC Press: Boca Raton, FL, 1998.
(46) Guo, X. J.; Wu, Z. J.; He, M. C. Removal of antimony(V) and antimony(III) from drinking water by coagulation−flocculation−sedimentation (CFS). *Water Res.* **2009**, *43*, 4327−4335.
(47) Meng, X. G.; Bang, S.; Korfiatis, G. P. Effects of silicate, sulfate, and carbonate on arsenic removal by ferric chloride. *Water Res.* **2000**, *34*, 1255−1261.
(48) Meng, X. G.; Korfiatis, G. P.; Bang, S. B.; Bang, K. W. Combined effects of anions on arsenic removal by iron hydroxides. *Toxicol. Lett.* **2002**, *133*, 103−111.
(49) Zeng, H.; Fisher, B.; Giammar, D. E. Individual and competitive adsorption of arsenate and phosphate to a high-surface-area iron oxide-based sorbent. *Environ. Sci. Technol.* **2008**, *42*, 147−152.
(50) Voegelin, A.; Kaegi, R.; Frommer, J. Effect of phosphate, silicate, and Ca on Fe(III)-precipitates formed in aerated Fe(II)- and As(III)-containing water studied by X-ray absorption spectroscopy. *Geochim. Cosmochim. Acta* **2010**, *74*, 164−186.
(51) Schwertmann, U.; Cornell, R. M. *Iron Oxides in the Laboratory*, 2nd ed.; VCH: Weinheim, Germany, 2000.
(52) Luo, X. B.; Wang, C. C.; Luo, S. L. Adsorption of As(III) and As(V) from water using magnetite Fe_3O_4-reduced graphite oxide−MnO_2 nanocomposites. *Chem. Eng. J.* **2012**, *187*, 45−52.
(53) Ruan, H. D.; Frost, R. L.; Kloprogge, J. T.; Duong, L. Infrared spectroscopy of goethite dehydroxylation: III. FT-IR microscopy of in situ study of the thermal transformation of goethite to hematite. *Spectrochim. Acta A* **2002**, *58*, 967−981.
(54) Song, S.; Lopez-Valdivieso, A.; Hernandez-Campos, D. J. Arsenic removal from high-arsenic water by enhanced coagulation with ferric ions and coarse calcite. *Water Res.* **2006**, *40*, 364−371.